Letter

# Feasibility of a small-scale test apparatus in measuring blast intensity of shallow buried charge detonation in in-situ soil

Zulkifli Abu Hassan*†, Aniza Ibrahim*, and Norazman M. Nor*

*National Defence University of Malaysia, Sungai Besi Camp, 53100 Kuala Lumpur, MALAYSIA
Phone: +603-9051-3400
†Corresponding author: 3080329@alfateh.upnm.edu.my

Received: March 12, 2018 Accepted: August 28, 2019

## Abstract

In this project, a robust portable apparatus has been developed for the use to quantify the effect of in-situ tropical soil properties and ejecta on blast loadings. In the effort to substantiate the efficacy of the apparatus in measuring blast loading of a shallow buried explosive in soil at natural condition, series of small-scale air blast tests and detonation of shallow buried explosive in silica sand have been carried out. Two methods of measurement were employed, namely the optical method and instrumentation method, where data with regard to test apparatus flight time, peak height, and peak acceleration of the target plate were obtained. Repeatability in obtaining the measured data are important as it suggested the feasibility of the test apparatus. Results from both measurements in optical and instrumentation methods have shown less than 10% in data variations from the average value. This signified the capability of the apparatus to provide consistent measurement during the tests. Another important aspect of the test apparatus is its ability to provide data on the effect of ejecta through measurement of target plate acceleration.

***Keywords***: buried explosive, small-scale experiment, in-situ soil test, blast intensity, soil ejecta



## 1. Introduction

Properties and conditions of the soil that are crucial in causing variation of magnitude and intensities of blast loads have been identified and presented in many documented researches[1)-4)]. Soil properties and conditions such as moisture content, particle size distribution, density and depth of burial (DoB) of the explosive charge are reported to be key dependent factors in causing variations in blast intensity of a landmine explosion[5),6)]. Since then attempts to quantify landmine blast loading have seen many developments of testing facilities and apparatus. The main objective is to mitigate the effect of close-range landmine blast impact, the experimental study varies from investigating integrity, modification, design and safety of the structure, and ultimately the safety of humans who are the occupants contained by the structure.

Facilities are developed mostly to conduct full-scale testing on vehicle protection validation testing, commonly comply to blast threat level described in the Allied Engineering Publication (AEP-55)[7)] or RSA-MIL-STD-37[8)]. The AEP-55 specifies blast threat level 2 to 4 for anti-tank mines as defined in STANAG 4569, specifying 6 kg, 8 kg and 10 kg TNT explosive mass respectively. Approach in RSA-MIL-STD-37 on the other hand, stated only one threat level which specifies the use of 8 kg TNT explosive mass.

Many of the landmine blast testing facilities feature large and heavy permanent structures[9)-12)]. These facilities are used to conduct full-scale tests on landmine blast utilizing explosive charge mass range up to 6 kg to 8 kg TNT. Comparatively, small-scale experimental tests can be conducted on smaller facilities, the apparatus and the amount of explosive mass were relatively scaled according to the same requirements[13)]. As confirmed by comparison between experimental and numerical results[14)], with appropriate magnification factor, a small-scale test can be successfully applied to assess structural dynamic response subjected to a close range buried explosion[15),16)].

Experimental blast tests to assess soil properties effects

on buried mines blast impulse, nevertheless, have been conducted in similar manner[6), 17)–19)]. Almost all of these facilities conducted buried mine tests where explosive charge were buried in remoulded soil test-bed or in a container. The present study was carried out to substantiate the efficacy of the apparatus that will be used in measuring soil blast effects in its natural condition. The outcome anticipated from this experiment is to access whether the proposed method and apparatus would be able to measure blast output in repeatable manner and consistent with the hypotheses in detonation of both in air-blast and blast-in-sand. Therefore, the efficacy depends on repeatability of results in both test setups. Apart from repeatability, robustness of test apparatus in undergoing numerous blast tests, and ease of mobilization of the test apparatus to various testing sites, would be the main criteria of considerations.

## 2. Design of the apparatus

In this study, a test apparatus has been developed to measure a close-in explosion of a high explosive detonation where the stand-off distance would be in the range within the fire-ball. For the purpose of multiple testing, it is not practicable to use direct measurement method using instrumentations. Possible way to measure is through structural response during the blast event. Thus, the blast output was measured by mean of optical method using hi-speed video camera, and instrumentation by piezoelectric shock accelerometers through the response of the test apparatus.

The test apparatus comprises of a steel test jig, steel target plate and instrumentations which may consist of a number of electronic sensors depend on testing requirements. There will be no permanent infrastructure required for the experimental set-up, the apparatus is developed in such that it is portable, easy to set up at test sites, and can be used in multiple testing. The influence of soils on landmine blast intensity will be measured by sensors and test apparatus responses during the instance of the blast.

The apparatus is modelled at a scale of 1/10$^{th}$ (scale factor 10) to represent the undercarriage dimension and weight of an armoured vehicle. The underside dimension of the apparatus however, is made into a square shape instead of rectangular. This is attributed to the purpose of maximising the receiving impact from buried explosive blast by the target plate, the apparatus is shown schematically in Figure 1.

### 2.1 Test jig

The main structure of the test jig is made up from a C-section mild steel structural channel with 100 mm web × 56 mm flange × 5 mm thickness (Figure 2). Four pieces of the C-section mild steel members are welded and bolted together to form a square frame of 500 mm × 500 mm size with a square opening of 390 mm side in its centre. The bottom side of the frame is where a 500 mm × 500 mm steel target plate is attached. The test jig is supported by adjustable steel legs that are fixed at the four corners of the steel frame. This allow the adjustment to be made to gauge the required gap of a stand-off distant, that is between the ground surface and the face of the target plate. The complete assembly of the apparatus weighed about 21.74 kg or representing 21.74 tons on a full-scaled prototype. The test apparatus is fitted with accelerometer adapter, pressure gauge adapter and LVDT casing, these instrumentations can be fixed on the apparatus based on the project requirements. However, in this particular experiment LVDT and pressure gauge were opted out.

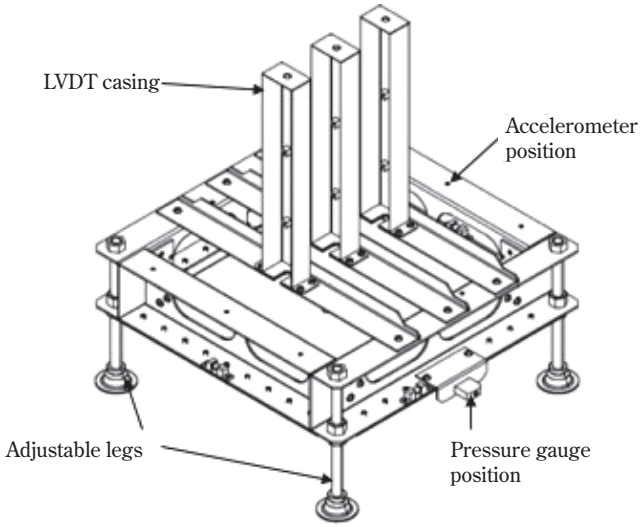


**Figure 1** Schematic drawing of the test apparatus.

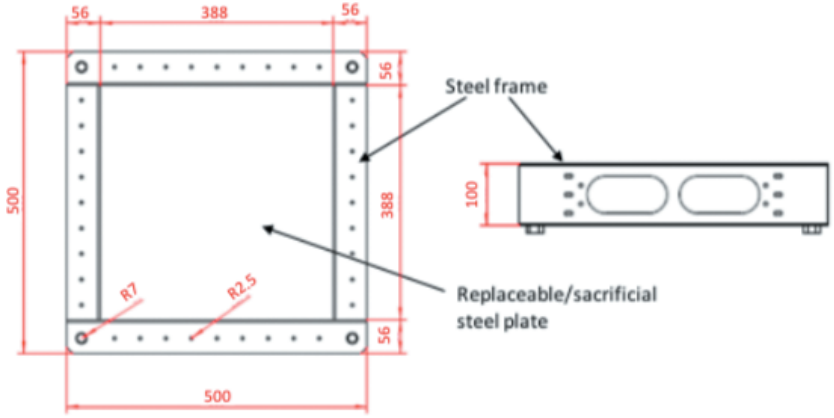


**Figure 2** Schematic drawing of the steel frame.

### 2.2 Target plate

The target plate that is used in the experiment is a sacrificial replaceable steel plate, as it is anticipated for a plastic impact. It is a 500 mm × 500 mm with 5.0 mm thickness mild steel plate. The plate is attached at the bottom face of the frame by being bolted with 36 tensile bolts. Upon installation, the target plate is allowed to move free under the blast load, which is made available by a 390 mm × 390 mm square opening of the frame. An adapter for accelerometer is mounted on the top face of the target plate, positioned at 80 mm from the centre of the plate.

## 3. Measurement methods

### 3.1 Optical method

Optical method was opted to measure the response of the test jig, for this purpose Phantom V series high-speed video camera was used and shot at the speed of 30000 frame per second. The camera was positioned approximately 5.0 m from the test apparatus during the blast test.

Optical method allows determination of initial velocity values through 'half-flight' translation which refers to vertical upward movement of the jig until it reaches the peak height, and 'full-flight' of the jig which include the vertical upward movement of the jig until it reaches the peak height and its vertical downward movement until it reaches the ground. By using two typical equations, calculation for initial velocity values are attainable[19]. Initial velocity $v_o$, based on half-flight translation is given by Equation (1).

$$v_o = \frac{(s_2 - s_1) + \frac{1}{2}g\left(t_2^2 - t_1^2\right)}{t_2 - t_1} \tag{1}$$

Where $s_1$ is the jig position at start and $s_2$ is position at peak height, corresponding recording times $t_1$ is time at start, and $t_2$ is time as it reaches peak height.

For initial velocity based on full-flight of the jig, it is determined from its initial position to the last position when it fall back to where it starts. If $t_f$ is the time when it started to move vertically upwards to the time when it fall back to its starting position, $g$ is gravitational constant equal to 9.81 m·s$^{-2}$, and $\theta$ is angle of upwards translation, therefore, $v_o$ is a result from Equation (2).

$$v_o = \frac{t_f g}{2\,\mathrm{Sin}\theta} \tag{2}$$

Though it seemed redundant to calculate initial velocities in both half and full-flight, the effort was to narrow the observation error in optical method. From optical method observation, Energy transfer can also be obtained by using Equation (3).

$$\text{Energy transfer} = mgh \tag{3}$$

Where $m$ is the mass of apparatus, $g$ is acceleration due to gravitational force, and $h$ is the peak height reached by the apparatus.

### 3.2 Accelerometer

There are three sensor devices that can be attached to the test apparatus, either mounted on the target plate, or on the steel frame. In the present work, only one piezoelectric accelerometer was used to measure the acceleration of the steel target plate. It was mounted on an adapter that is welded on the target plate located 80.0 mm from the centre of the plate. This accelerometer employs PCB Piezotronic ICP shock accelerometer which can be calibrated up to 10 kHz with maximum acceleration measurement range up to 50000 G's pk (490000 m·s$^{-2}$).

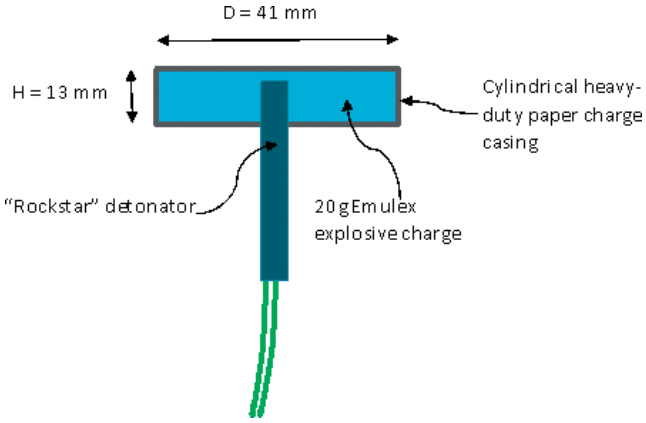


**Figure 3** Explosive charge assembly.

## 4. Explosive charge

Each of the blast test in this experiment was conducted by detonating the mass of 20 g AN Emulsion High Explosive commercial grade explosive charge, it has density between 1.13 g·cc$^{-1}$ to 1.24 g·cc$^{-1}$ and relative bulk strength of 109. The velocity of detonation (VOD) of Emulex is between 4500 to 5500 m·s$^{-1}$ with explosion energy around 2.85 MJ·kg$^{-1}$. The explosive was detonated using detonator containing secondary charge mass of 720 mg PETN. The equivalent of the total charge mass is 19.19 g of TNT, this was based on conversion proposed by Locking[20], which is given by Equation (3). Hopkinson's scaling law also applies to the mass of explosive charge.

$$\text{TNT Equivalent} = Q_{EXP}/(Q_{TNT}\,(1-d) + m \cdot Q_{EXP}) \tag{4}$$

where, $Q$ = heat of detonation, $d$ = 0.76862 (line intercept), and $m$ = 0.7341 (line gradient).

The explosive charge was moulded into a disc-shape charge using heavy-duty paper casing, with a height to diameter (H/D) ratio of approximately 0.33. This ratio adapts to the surrogate anti-tank landmine shape described in AEP-55. Detonator is inserted from the bottom at the centre of the disc-shape charge to approximately half depth of the charge. The assembly of the explosive charge is shown in Figure 3.

## 5. Test setup

In order to assess the efficacy of this method and the apparatus, detonation tests were carried out in two different setups, namely an air-blast setup, and buried-in-sand setup. The reason being for these two setups were chosen is because of the test's repeatability with respect to the transmission of blast output. With constant stand-off distance and constant mass of explosive charge, a

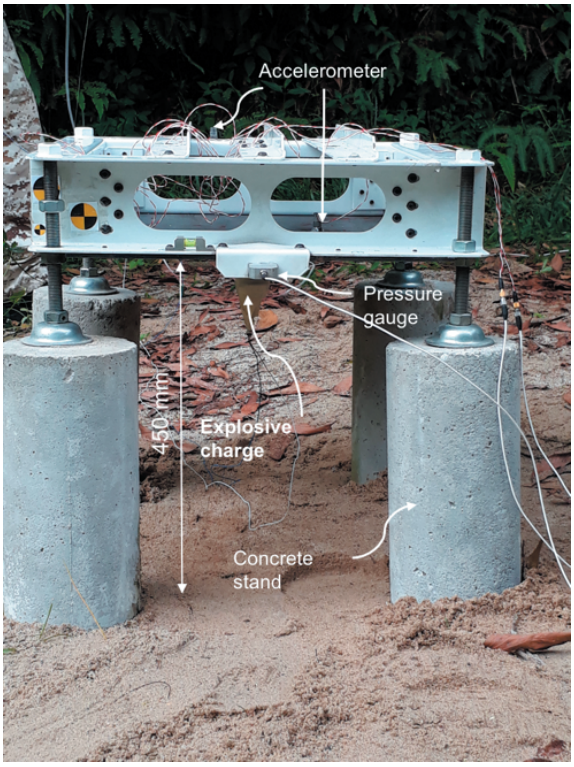


**Figure 4** Experimental setup for air-blast test.

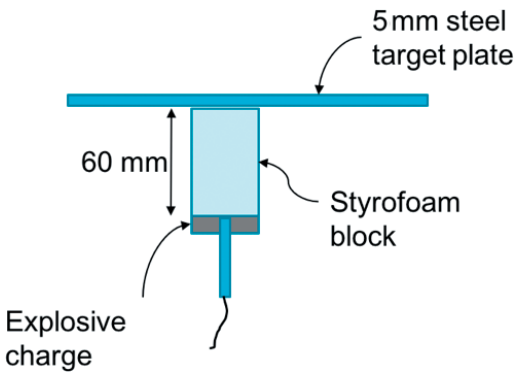


**Figure 5** Explosive charge positioned facing the target plate by sticking on polystyrene spacer block.

detonation in the air will likely to give similar blast output. For the case of buried explosive, charge buried in sand with uniform particle size distribution would also give repeatable results when the condition of the stand-off distance, depth of burial, and mass of explosive charge are constant throughout the test[4].

### 5.1 Air-blast test setup

In the air-blast test (AT test), test apparatus was placed with its adjustable legs sat on four of concrete stands. In order to prevent possibility of ground reflected blast wave from affecting the measurement, the height between the ground surface and the face of the target plate is set at about 450 mm (Figure 4). The explosive charge was secured to a 60 mm height polystyrene spacer block, the other end of this block was mounted at the centre of the face of the target plate as shown in Figure 5. The polystyrene block is assumed weightless, and to ensure a constant stand-off distance for air blast.

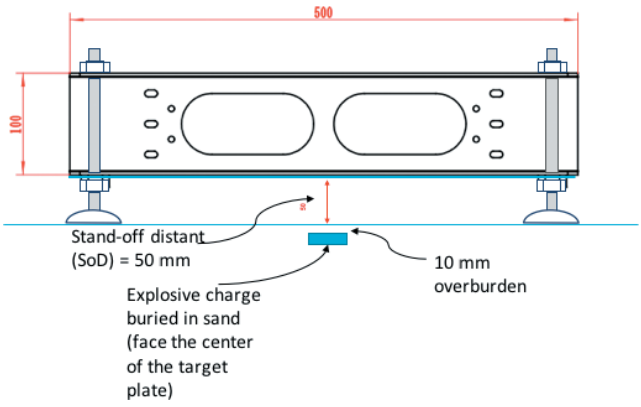


**Figure 6** Position of the apparatus and explosive charge in the buried explosive test setup.

### 5.2 Buried-in-sand test setup

This experiment used silica sand as embedded material for buried explosive. In the buried-in-sand test (ST test) setup, test apparatus was place standing on the ground on the silica sand test bed. The height of the apparatus with respect to the target plate was controlled to specific height by adjustable legs. The height is set to the stand-off distant (SOD) of 50 mm. SOD in this test is defined from the face of the target plate to the surface of the ground. Explosive charge was buried in the test bed at a position aligned to the centre of the target plate. The depth from the top surface of the explosive to the surface of the ground was specified at 10 mm, this distant is defined as the depth of overburden of the soil cap. The test setup for buried explosive is shown in Figure 6.

## 6. Results and discussion

### 6.1 Optical method test results

The test jig response from the time when it was launched vertically upwards to the peak height until it dropped freely back to the point it started was observed. In the AT tests, peak heights reached are between 53 mm and 60 mm, with the average peak height spot at 56 mm and the variations in peak height spread at the highest of 7% from the average. The average time when peak heights are reached which is also the average half-flight time is 0.095 s. Half-flight time varied between 0.088 s and 0.103 s, their variations spread at the highest of 8% from the average. For a full-flight time, average total flight time for AT tests lasts for 0.19 s and its highest spread lies within 6% of the average. While for the ST tests, peak heights reached between 222 mm and 253 mm, averaging at 245 mm, and highest spread in peak height is about 9% from the average. From three ST tests, the average half-flight time is 0.21 s and varied with highest spread about 9% from the average. Total flight time ends at 0.4 s and its highest spread occurs at 7% of the average. Both AT and ST tests peak height are shown in Figure 7.

It was obvious that the higher the jig translated upwards the longer it took in flight. The time taken in the ST tests for the jig to reach both its point of peak height and back to the starting point from where it was initially translated is twice longer than in AT tests. However, the average peak height in AT tests is around 56 mm while

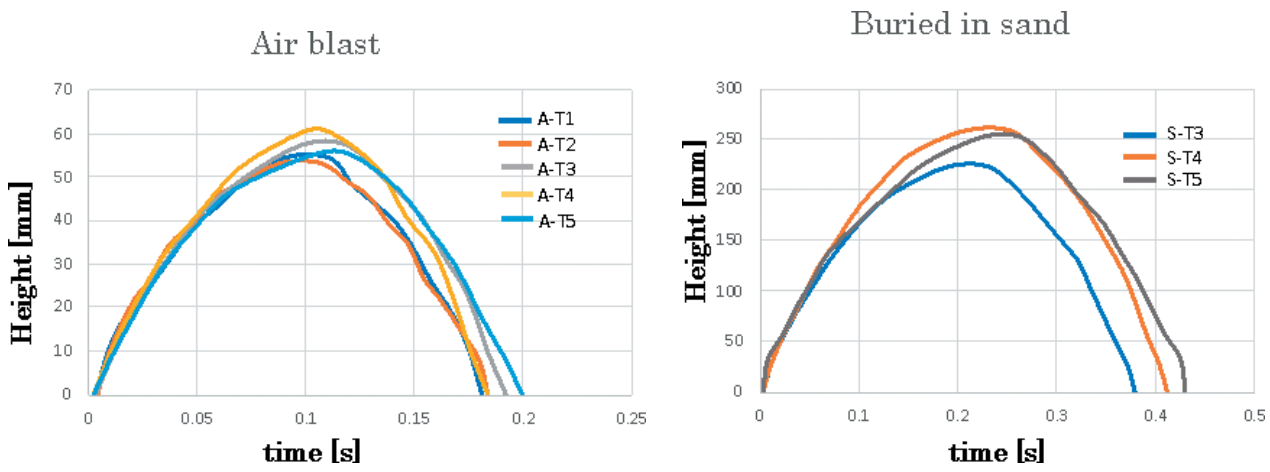


Figure 7 Jig flight height time history.

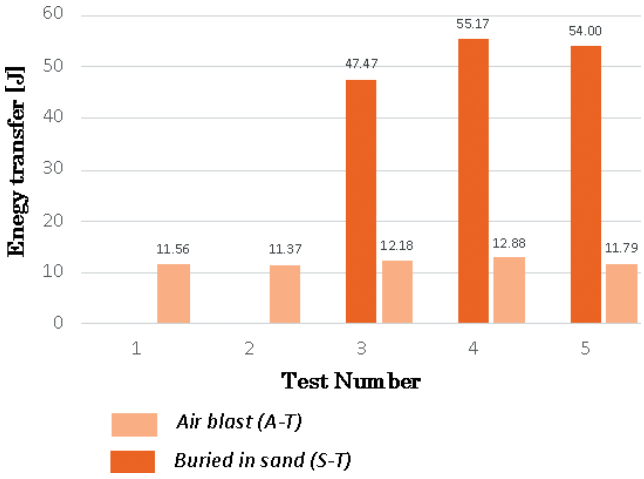


Figure 8 Comparison of total energy transfer in AT and ST tests.

the average peak height reached about 245 mm in ST tests, this is almost 4 times higher than in AT tests. Based on Equation (3), at a constant gravitational acceleration g, the potential energy of a mass is the function of its height, this also mean that the energy transferred from the explosion to the jig is 4 times higher in ST tests. Figure 8 shows that buried explosion in ST tests transfers in average of 52.2 J of energy from the explosive to the jig resulting the jig to move vertically upwards 4 times higher than the height in air-blast AT tests which recorded only 12 J of average energy transfer.

Velocity measurement was also made possible through the optical observation of flight-time history. Two means of calculation were adopted which included half-flight and full-flight of the jig. Figure 9 shows initial velocities of half-flight and full-flight in both AT and ST tests, based on calculation using Equation (1) for half-flight and Equation (2) for full-flight. In the AT and ST tests, half-flight observation gives higher initial velocity values compared to the full-flight observation. The AT tests half-flight initial velocity averages at 1.06 $m \cdot s^{-1}$ and 0.92 $m \cdot s^{-1}$ for full-flight, from both averages of flights velocities give the AT test mean initial velocity of 1.0 $m \cdot s^{-1}$. While average initial velocity in the ST tests, half-flight and full-flight are 2.2 $m \cdot s^{-1}$ and 2.0 $m \cdot s^{-1}$ respectively, this would give mean initial velocity of 2.1 $m \cdot s^{-1}$. As noticed earlier in the flight height-time history, total flight time in ST tests is twice longer than the AT tests total flight time. Since the initial velocity is the function of flight distance and time, it is anticipated that the initial velocity values in ST tests would also be twice greater than the AT tests.

However, in both AT and ST tests, initial velocities values are higher in half-flight calculation compared to full-flight. The reason it was higher because flight time calculated in half-flight is from the moment the jig started to move upward to the first instance it reached the peak height. From the observations, impulse transferred from the blast load forced the apparatus to vertically displace, but when it moves further upwards the momentum begin to subside as it reached peak height. At the peak height, it was noticed that the jig floats about 20 ms before exhausted. Shortly after that it started to drop in a free-fall manner which is almost at the same rate when it was rapidly forced upwards. The floating time was accounted in the total flight time but not in half-flight time, therefore influence the initial velocities value in half-flight calculation.

## 6.2 Accelerometer results

Results presented are based on measurement data obtained using piezoelectric accelerometer mounted at the back face of the target plate, located 80 mm from the centre point of the plate. Four numbers of reading were obtained in the AT tests, namely test 1, 2, 3, and 5. In the ST tests only two readings were acquired from test 4 and 5.

From piezoelectric accelerometer data, acceleration of the target plate subjected to blast loading were recorded. Figure 10 shows plate acceleration time histories of the AT and ST tests. The average peak acceleration in AT tests lies at 13000 G, and highest variations of peak point in AT tests spread about 8% from the average value. In the ST tests, peak accelerations were also recorded between 1 and 2 ms, peak acceleration averages at 12550 G, and variation of both peaks is 7.6% from the average. The graph patterns however were distinguished from AT tests by two peaks of sudden surge. After the first peak, another rapid surge occurred once again when the time past between 5 and 10 ms, it surges between 1400 and

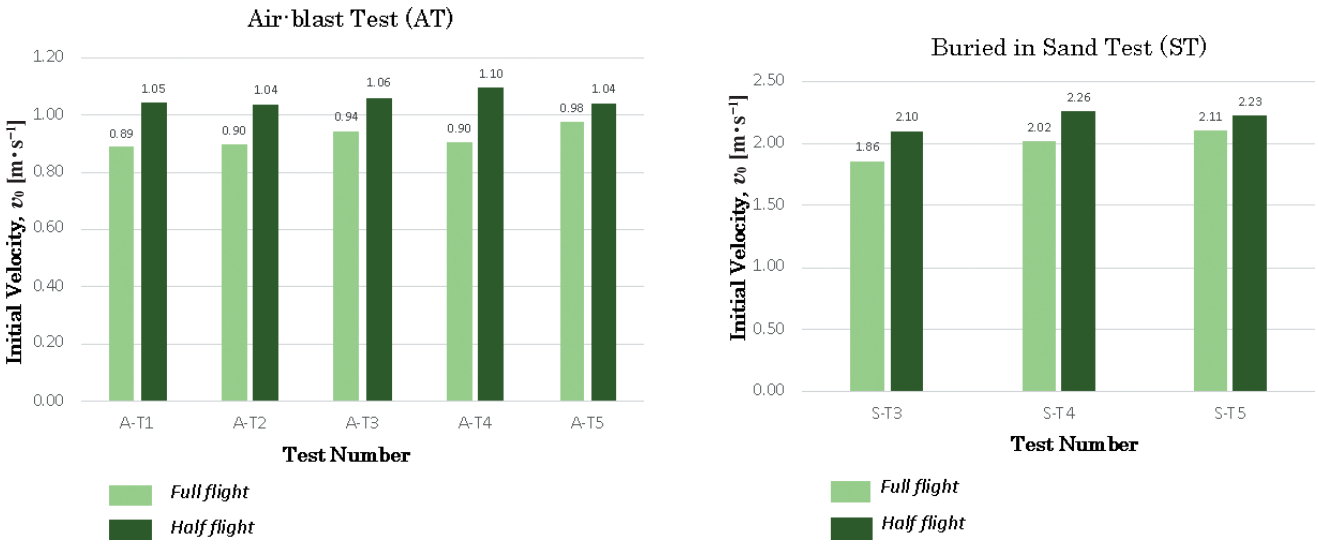


**Figure 9** Comparison of initial velocity for full-flight and half-flight.

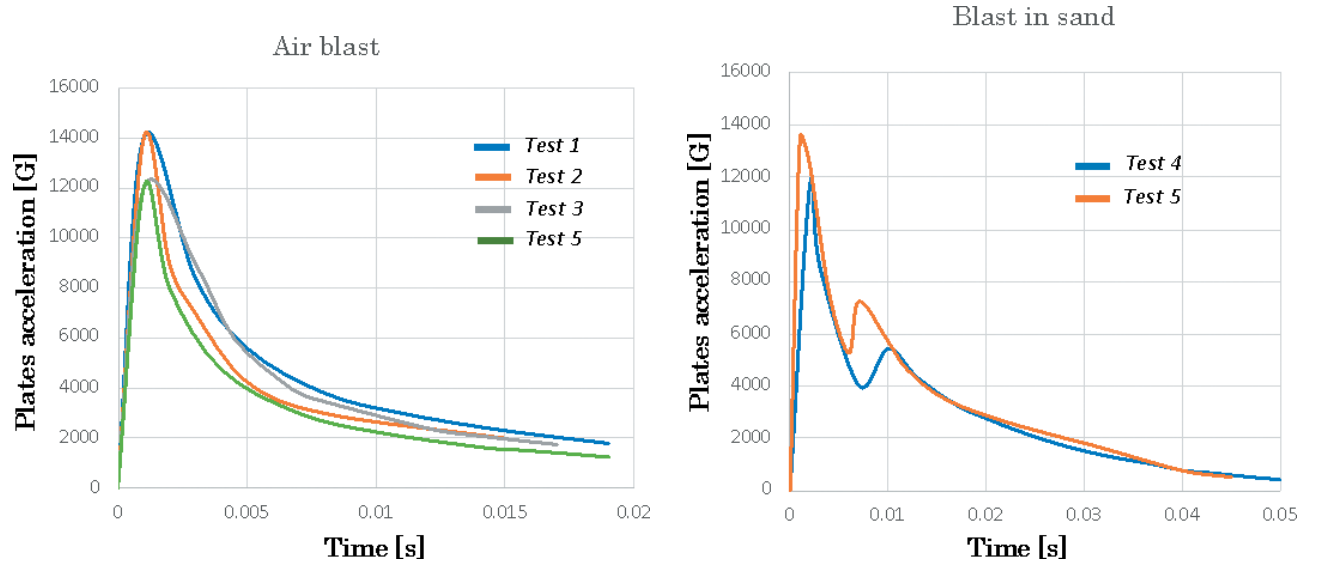


**Figure10** Plate acceleration-time history at 80 mm from centre of target plate.

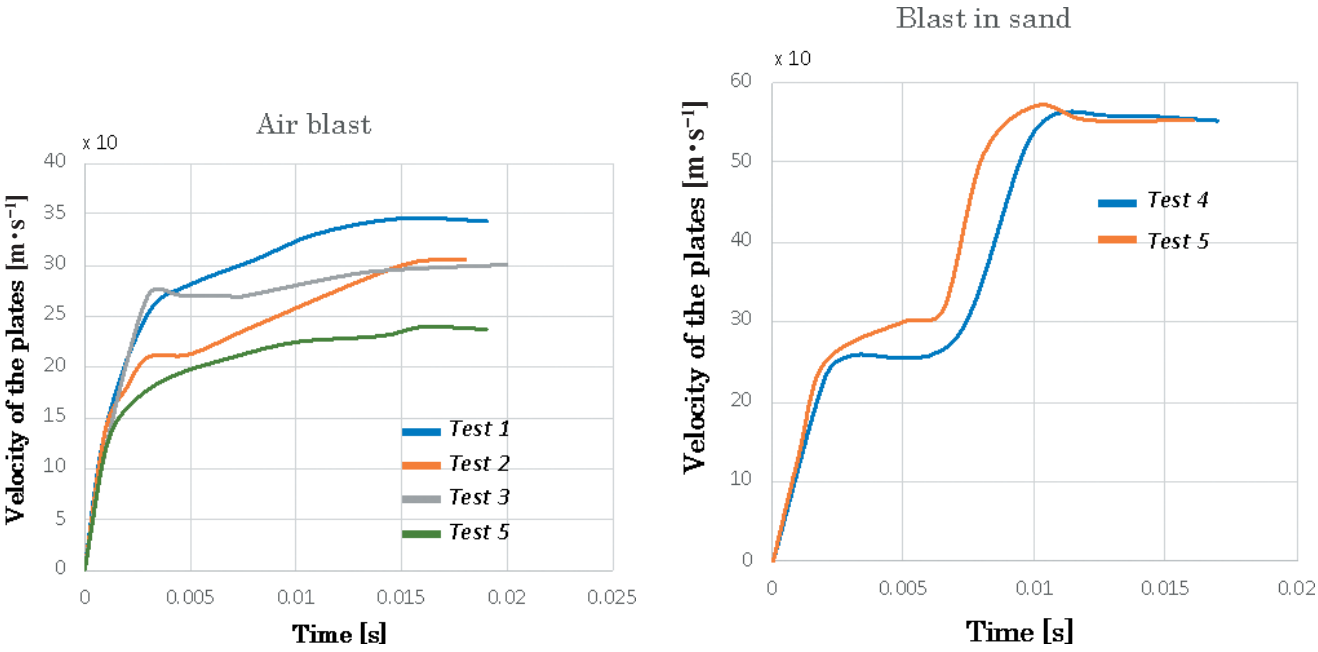


**Figure11** Plate velocity-time history.

2000 G in test 4 and 5 respectively, before continuing to steadily decline in acceleration.

It is interesting to note that the time between 5 and 10 ms coincided with the boundary of gas expansion phase and ejecta phase of blast evolution in soil[21]. This also suggested that the surge of acceleration could be due to the effect of soil ejecta impacting the target plate. It is very important to be able to capture this because different soil types and conditions may (are likely to exhibit) have different magnitude of surges and profiles.

The plate although experiencing blast impact and acceleration, at the same time is moving upwards together with the apparatus. Although peak accelerations were recorded from 1 ms, the observation made through hi-speed camera showed that as the time past 0.23 ms, deformation of the target plate has already taken place where its surface has beginning to bulge, and the apparatus started to move upwards at about 1.56 ms. In contrast with the recorded acceleration, the moment the apparatus was about to translate upwards, the plate acceleration has already beginning to enter its receding phase.

Velocities of the target plate time histories in AT and ST tests is shown in Figure 11. Velocities in AT tests peak at around 15 ms with average velocity gets as high as 300 $m{\cdot}s^{-1}$. Velocity-time history in ST tests have distinct pattern compared to AT tests, where there are two instances of velocities upsurge. The first 1 ms may look similar to AT tests, velocities were seen to get constant as it passed 3 ms and reached in average of 285 $m{\cdot}s^{-1}$ at 5 ms. However, at 6–7 ms, velocities started to rapidly rise again before getting into constant velocity and peak at around 10 ms with average velocity of 550 $m{\cdot}s^{-1}$.

When comparing peak acceleration in AT and ST tests, the average peak acceleration in both tests did not differ much in value, where the average of both tests plate acceleration was around 13000 G. Nevertheless, data in terms of velocity showed better indication of the blast impact received by the target plate. Plate velocity was almost twice higher in ST tests compared to in AT tests, although the first peak velocity may be almost similar, but possible impact from ejecta has resulted higher peak velocity in ST tests. Similar phenomenon was also acknowledged by Rigby et. al.[18] in experimental test using apparatus consisting array of Hopkinson pressure bar to measure direct loading from detonation of a buried explosive.

## 7. Conclusions

It was found that the two methods have shown encouraging results in fulfilling and accommodating the intended purposes of the apparatus, tests data in both optical and instrumentation methods have shown variation in less than 10% from the average value at specific key locations which suggested the capability of the apparatus to provide consistent measurement. Results also showed agreement with previous findings that buried landmine imparts greater blast impulse compared to in air blast, where from optical observations, energy transfer was 4 times higher in explosive buried in silica sand compared to air blast tests while instrumentation method recorded average plate velocity in buried explosion was twice greater than in air blast tests.

Another important indication of the apparatus plausibility is the distinct observable profiles exhibited in ST tests, where there is a clear shoulder between two steeps velocity upsurge occurred in ST tests. The first sudden increase in velocity was similar to those of AT tests, which is caused by blast wave and detonation products. However, it was followed by another rapid rise after about 4 ms of constant velocity, which is likely due to soil ejecta impacted the target plate. This indicate that the effect of ejecta in contributing towards the increment of blast magnitude can be determined through the response of the apparatus target plate. Results of the experiment therefore imply the feasibility of the apparatus to be used in obtaining near-field blast output data of buried explosive and effect of ejecta in in-situ soil blast effects.

## References


1) S. D. Clarke, J. Warren, and A. Tyas, Proc. 14th International Symposium on Interaction of the Effects of Munitions with Structures, Seattle, US (2011).
2) S. L. Hlady, Proc. 18th International Symposium on Military Aspects of Blast and Shock (MABS18), Bad Reichenhall, Germany (2004).
3) S. D. Clarke, S. D. Fay, J. A. Warren, A. Tyas, S. E. Rigby, and I. Elgy, Meas. Sci. Technol., 26, 1–13 (2015).
4) S. D. Clarke, S. D. Fay, J. A. Warren, A. Tyas, S. E. Rigby, J. J. Reay, and R. Liversey, International Journal of Impact Engineering, 274–283 (2015).
5) L. C. Taylor, R. R. Skaggs, and W. Gault, International Journal for Blasting and Fragmentation, Fragblast, 9, 19–28 (2005).
6) J. Q. Ehrgott, S. A. Akers, J. E. Windham, D. D. Rickman, and K. T. Danielson, Shock and Vibration, 18, 857–874 (2011).
7) NATO, Allied Engineering Publication (AEP) 55, Vol 2: Procedures for Evaluating the Protection Level of Logistic and Light Armoured Vehicles (for Mine Threat) (2006).
8) S. Nell, RSA-MIL-STD-37: Landmine Protected Wheeled Vehicles-Design, Development and Evaluation, Issue 3 (2000).
9) J. D. Reinecke, I. M. Snyman, R. Ahmed and F. J. Beetge, Proc. 2nd CSIR Biennial Conference Science Real and Relevant, Pretoria (2008).
10) P. M. De Koker, N. Pavkovic, J. T. Van Dyk, and I. Steker, Proc. International Symposium on Humanitarian Demining, Sibenik, Croatia, 31–39 (2009).
11) K. Williams, S. McClennan, R. Durocher, B. St-Jean, and J. Tremblay, Proc. 7th LS-DYNA Users Conference, 35–44 (2002).
12) A. Bouamoul, F. F. Gourdeau, G. Toussaint and R. Durocher, Defence R&D Canada, Valcartier Research Centre (2014).
13) N. Bochorishvili, N. Chikhradze, E. Mataradze, and I. Akhvlediani, IOP Conference Series: Earth and Environmental Science, 44, 1–7 (2016).
14) A. Neuberger, S. Peles and D. Rittel, International Journal of Impact Engineering, 34, 874–882 (2007).
15) X. Zhao, G. Shultis, R. Hurley, M. Sutton, W. Fourney, U.

Leiste, and X. Deng, Experimental Mechanics, 539–555 (2014).
16) X. Zhao, R. Hurley, M. Sutton, W. Fourney, U. Leiste, and X. Deng, Experimental Mechanics, 556–568 (2014).
17) S. D. Fay, S. D. Clarke, A. Tyas, J. Warren, S. Rigby, T. Bennett, I. Elgy, and M. Gant, Proc. 23rd International Symposium on Military Aspects of Blast and Shock, Oxford (2014).
18) S. E. Rigby, S. D. Fay, S. D. Clarke, A. Tyas, J. J. Reay, J. A. Warren, M. Gant, and I. Elgy, International Journal of Impact Engineering, 96, 89–104 (2016).
19) V. Denefeld, N. Heider, and A. Holzwarth, Defence Technology, 1–9 (2017).
20) P. M. Locking, Proc. 26th International Symposium on Ballistics, Miami, FL, USA (2011).
21) D. Bergeron, R. Walker, and C. Coffey, Technical Report 668, Defence Research Establishment Suffield, Ralston, Alberta, Canada (1998).